

EcoFed: Efficient Communication for DNN Partitioning-based Federated Learning

Di Wu, Rehmat Ullah, Philip Rodgers, Peter Kilpatrick, Ivor Spence, and Blesson Varghese

Abstract—Efficiently running federated learning (FL) on resource-constrained devices is challenging since they are required to train computationally intensive deep neural networks (DNN) independently. DNN partitioning-based FL (DPFL) has been proposed as one mechanism to accelerate training where the layers of a DNN (or computation) are offloaded from the device to the server. However, this creates significant communication overheads since the activation and gradient need to be transferred between the device and the server during training. While current research reduces the communication introduced by DNN partitioning using local loss-based methods, we demonstrate that these methods are ineffective in improving the overall efficiency (communication overhead and training speed) of a DPFL system. This is because they suffer from accuracy degradation and ignore the communication costs incurred when transferring the activation from the device to the server. This paper proposes EcoFed – a communication efficient framework for DPFL systems. EcoFed eliminates the transmission of the gradient by developing pre-trained initialization of the DNN model on the device for the first time. This reduces the accuracy degradation seen in local loss-based methods. In addition, EcoFed proposes a novel replay buffer mechanism and implements a quantization-based compression technique to reduce the transmission of the activation. It is experimentally demonstrated that EcoFed can significantly reduce the communication cost by up to 114x and accelerates training by up to 25.66x when compared to classic FL. Compared to vanilla DPFL, EcoFed achieves a 13.78x communication reduction and 2.83x training speed up.

Index Terms—Edge computing, Federated learning, DNN partitioning, communication efficiency

1 INTRODUCTION

Federated learning (FL) is a privacy-preserving machine learning paradigm that facilitates collaborative training without transferring raw data from participating devices to a server [1]–[3]. However, running FL training on resource constrained devices is challenging since training deep neural networks (DNN), which is computationally expensive, is solely run on devices. This is a known bottleneck [4]–[8].

DNN partitioning-based FL (DPFL) in which the DNN is partitioned across the device and server has been developed to surmount the challenge of running FL on resource constrained devices [9]–[11]. In DPFL, an entire DNN model is partitioned into two parts, i.e., a device-side model and a server-side model. The first few layers of the DNN are deployed on the device-side for training. The remaining layers are offloaded to a server that has more computational resources than the device. The computational burden on the device is alleviated as it only trains a few layers of the entire model. Consequently, the training time is significantly reduced.

Although DPFL reduces training time compared to FL, it incurs additional communication overheads. This is because the outputs of the activation generated by the device-side model in a forward pass and the corresponding gradients calculated during backpropagation need to be transferred

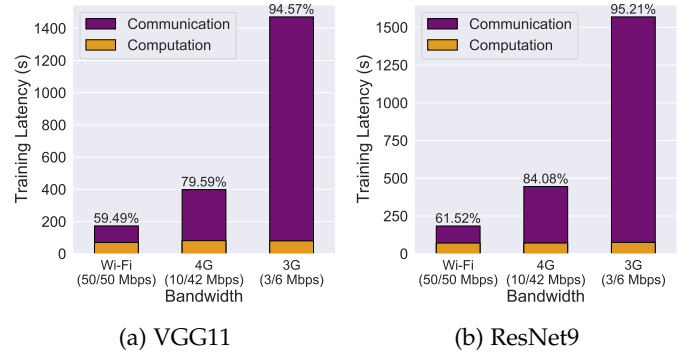


Fig. 1: Computation and communication latency in DPFL training under different network bandwidths. Numerical value above the bars is the percentage of communication latency.

between the devices and the server. Figure 1 shows the computation and communication latency incurred during DPFL training on the CIFAR-10 dataset with a batch size of 100 samples using an edge server (a 2.5GHz 8-core Intel i7 processor with 16GB RAM) and a device (Raspberry Pi 4 Model B). It is noted that communication latency is a new bottleneck in DPFL; communication requires up to 60% of the overall training time under Wi-Fi conditions and around 95% for 3G bandwidth.

Split Federated Learning (SFL), which we refer to as *vanilla DPFL*, is the first FL work that partitions the DNN across the device and the server [12]. However, the communication overheads introduced by partitioning are not considered. Recent DPFL methods [10], [11], we refer to as *local loss-based DPFL*, use local loss generated by an

- D. Wu and B. Varghese are with the School of Computer Science, University of St Andrews, UK. Corresponding author: dwu217@st-andrews.ac.uk
- R. Ullah is with the Cardiff School of Technologies, Cardiff Metropolitan University, UK.
- P. Rodgers is with Rakuten Mobile, Inc., Japan.
- P. Kilpatrick and I. Spence are with the School of Electronics, Electrical Engineering and Computer Science, Queen's University Belfast, UK.

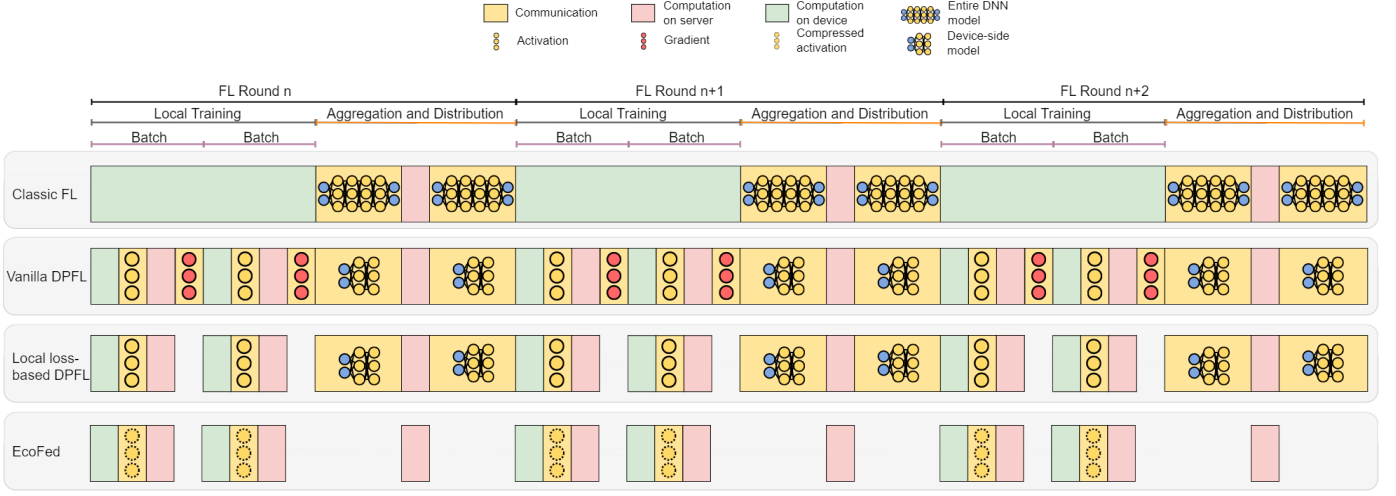


Fig. 2: The training pipeline of classic FL, vanilla DPFL, local loss-based DPFL and EcoFed for three rounds of training. Classic FL transfers the entire model from the devices to the server at the end of each round. Vanilla DPFL only needs to upload a partitioned device-side model at the end of each round. However, Vanilla DPFL transfers the activation and gradient for each batch sample. Local loss-based DPFL reduces the communication by half since the gradients are computed locally. EcoFed reduces communication further as it transfers the activation only periodically (for example, once in two rounds) and further compresses the size of the activations.

auxiliary network to train the device-side model instead of transferring and using the gradient from the server. Local loss-based DPFL can reduce half of the communication cost using device-side auxiliary networks since only the activation needs to be communicated from the devices to the server through the network.

Although local loss-based DPFL methods eliminate the communication of the gradient, we demonstrate that they cannot improve the efficiency of vanilla DPFL due to two significant issues (Section 4). Firstly, *The volume of communication required to achieve the target accuracy is not reduced and even increases due to poor learning performance observed by lower final accuracy and convergence speed.* The poor learning performance of local loss-based DPFL methods is referred to as ‘accuracy degradation’ that is caused by training using local loss instead of end-to-end training. We also demonstrate that the use of local error signals will lower the final accuracy and convergence speed (Section 4.3). As a result, the communication cost to achieve the target accuracy is similar to or even higher than vanilla DPFL (Section 4.4).

Secondly, *Under limited network bandwidth conditions, the training time does not significantly decrease since the upload bandwidth is usually lower than the download bandwidth.* Local loss-based DPFL methods do not consider the transmission of activation, which is significant - half of the communication volume and has a high frequency per iteration. Therefore, when the network bandwidth is limited, which is common in resource constrained environments, it is not feasible to accelerate training using current local loss-based DPFL methods (Section 4.5).

In this paper, we propose EcoFed, a communication efficient framework for DPFL on resource-constrained devices. Figure 2 illustrates the training pipeline of classic FL, vanilla DPFL, local loss-based DPFL and EcoFed. EcoFed only transfers the activation periodically (for example, once every two rounds) and further reduces the size of the activa-

tion, thereby reducing the overall frequency and volume of communication. Pre-trained initialization of the device-side model is employed in EcoFed to reduce accuracy degradation caused by local loss-based methods. The frequency of transferring activations is reduced by proposing a replay buffer mechanism in which the server-side model is periodically trained by making use of cached activations instead of regularly transferring the activation from the devices to the server. Moreover, EcoFed compresses the activation using a lightweight quantization technique to further reduce the size of the data transferred and the corresponding buffer. Two DNN models and datasets are considered in our evaluations by comparing EcoFed against four baselines, including classical FL, vanilla DPFL and two state-of-the-art local loss-based DPFL methods. EcoFed improves the test accuracy compared to the baselines while reducing the communication volume by up to 13.77x and thus accelerates training by up to 2.83x compared to other DPFL methods.

The **research contributions** of this paper are:

1) Identifying the limitations of local loss-based DPFL approaches by systematically exploring the accuracy, communication size and training latency of DPFL methods on resource constrained devices.

2) Designing, developing and evaluating EcoFed, the first framework to effectively reduce communication overheads of DPFL by proposing novel approaches that optimize the forward and backward passes in DPFL.

3) Proposing novel techniques that use pre-trained initialization on the device-side to eliminate the need for transferring gradients from the server to the device without significant accuracy degradation and a replay buffer along with quantization for reducing the frequency and volume of activations transferred to the server in DPFL.

The rest of this article is organized as follows: Section 2 provides an overview and the underlying methods of the EcoFed framework. Section 3 theoretically analyzes con-

vergence and the computation and communication cost of EcoFed. Section 4 evaluates EcoFed against the baselines. Section 5 presents the related work and Section 6 concludes this paper.

2 ECOFED FRAMEWORK

This section firstly provides an overview of the proposed EcoFed framework (Section 2.1). Then the underlying techniques, namely *Pre-trained Initialization* (Section 2.2) and *Replay Buffer* (Section 2.3) are presented followed by the proposed algorithm of EcoFed (Section 2.4).

2.1 Overview

Figure 3 provides an overview of the modules of the EcoFed framework that operates across resource constrained devices and servers (either cloud or edge servers). The underlying techniques used by the modules are discussed in the next sub-section.

When FL training begins, the *Initializer* (❶) module on the server determines the training scheme (the configurations of the DNN models) and initializes the weights. The *Initializer* also splits the model (to device-side and server-side models) for each participating devices. The device-side models are sent to the participating devices and the corresponding server-side models are sent to servers.

In vanilla DPFL, after configuration, the training starts on the device-side model for each device. The *Device Trainer* (the training engine on devices, ❸) will first generate activation outputs of the device-side model. The outputs and labels of the corresponding data samples are sent to the servers. The *Server Trainer* (the training engine on servers, ❷) trains the server-side model using the activation outputs received from the device and generates corresponding gradients. The gradients are sent back to each device to update the device-side model. The above steps are repeated for each batch sample in vanilla DPFL training.

However, in EcoFed, before generating and sending the activation outputs of the device-side model to servers, the *Activation Switch* (❷) will determine whether the outputs of the device-side model are required to be sent to the server or the server can use the buffer with the cached activation to train the server-side model. If the activation outputs are required to be sent, then they will be further compressed using the quantization technique implemented by the *Compressor* (❹). The compressed activation and labels of the corresponding samples will then be sent to the server. On the server, the compressed data will be firstly used to update the *Replay Buffer* (❺) and reconstructed by the *Decompressor* (❻) for training the server-side models. The *Server Trainer* only needs to calculate and update the gradients of the server-side models without sending the gradient back to each device for training the device-side models.

After completing the above steps, the *Aggregator* (❽) will collect updated weights from each device for aggregation and for generating new global weights using the *Federated Averaging* (FedAvg) algorithm [13].

EcoFed reduces the communication cost in vanilla DPFL by eliminating the transmission of the gradient, adjusting the communication frequency of the activation and compressing the activation data. The *Initializer* uses pre-trained

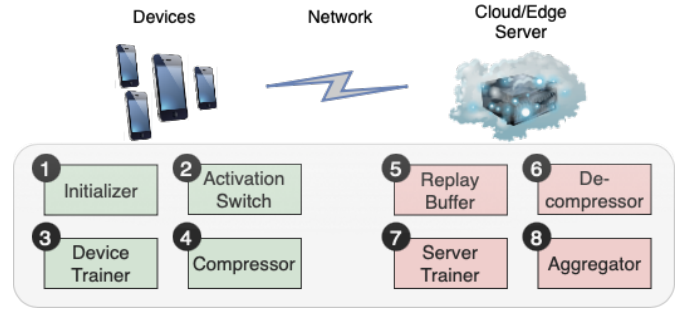


Fig. 3: EcoFed modules on the device and server.

weights to initialize the device-side model and freezes them during training, thus eliminating the need for transmitting the gradient. In addition, The *Activation Switch* periodically uploads the output activation of the device-side model to edge servers to update the *Replay Buffer*. When the edge server does not receive the activation from devices, it will continue training the server-side models using the activations that were cached in the *Replay Buffer*. The *Compressor* and *Decompressor* modules are underpinned by quantization and dequantization techniques based on those in the literature [14]–[16].

2.2 Pre-trained Initialization

Existing local loss-based DPFL incorporates local error signals to train the device-side model using an auxiliary network [10], [11], [17]. The auxiliary network consists of a few lightweight hidden layers, for example, fully connected layers that map the output of the device-side model to the same dimensions as of the ground truth labels. Although the local error signals eliminate the need to transfer global gradients from the server to devices, this approach adversely impacts accuracy and convergence rate since the device-side model and the server-side model are decoupled and trained by different error signals, namely local error signals and global error signals. We empirically demonstrate this in Section 4.3. A similar accuracy loss is reported in the literature for greedy layer-wise learning. In this method, the use of an auxiliary network results in accuracy degradation when compared to end-to-end training that uses global loss calculated with the entire model [18]. As a result, the communication required to achieve the target accuracy is effectively not reduced and even increases due to the lower accuracy and slower convergence speed of local loss-based methods.

To address the above, EcoFed adopts pre-trained initialization of the device-side model (w_C). The device-side model is initialized with pre-trained weights ($w_{C,k}$), which are the partial weights of the entire model trained on a large dataset (e.g. ImageNet [19]). In addition, we empirically study the impact of local loss on generating activation outputs, which are used to train the server-side model. We identify that local loss is not a satisfactory criterion for representing a ‘good’ activation output for training the server-side model with pre-trained initialization (Section 4.3). Therefore, during FL training, we freeze the weights of the device-side model ($w_{C,k}$), which runs the first few layers of

the model that learn general features. These layers are not specific to a particular task, and therefore, the weights of a pre-trained model can be transferred to another model [20]. In this paper, the weights are transferred to the device-side model.

Benefits of pre-trained initialization: There are four benefits to pre-trained initialization and freezing weights of the device-side model $w_{C,k}$ in the context of DPFL. They are: (i) Communication during training is reduced since the need for the devices to receive gradients from the edge server is eliminated; (ii) accuracy loss caused by using local error signals is reduced; (iii) the computational workload on resource constrained devices is reduced since the gradients of $w_{C,k}$ do not need to be calculated and updated on the devices; (iv) the device-side model ($w_{C,k}$) and the respective activation outputs are not significantly changed during each training round, making it possible to use cached activations from a buffer to train server-side models.

2.3 Replay Buffer

EcoFed introduces a *Replay Buffer* on the edge server, i.e., the server uses the activation cached in the buffer, which is obtained from a previous training round, to train the server-side model in a given round. EcoFed caches and updates the buffer periodically. If the transmission of activations is switched off in a given round, then EcoFed will reuse the cached activations. Therefore, there are two modes of training, namely EcoFed with and without the buffer.

Periodic transfer: The *Activation Switch* controls the transfer frequency of the activation in the forward pass from the device-side to the server-side model. The frequency is controlled by the interval between successive activation transfers, which is denoted as ρ . Consider, for example, $\rho = 2$. In this case, the activation outputs of the devices will only be transferred every second round and the buffer is cached with the activations when it is sent. During the other rounds, the edge server will use the cached activations to train the server-side models. It is worth noting that the activations (a_k^t) for each round will change due to different participating clients, data batches and data augmentations. Thus, the buffer on the edge servers needs to be periodically updated during the training. Thus, ρ is a hyper-parameter that will affect the model performance and communication cost of EcoFed, which is further considered in Section 4.3.

Reducing the buffer size: A potential issue that must be mitigated is that a large buffer may be required if large or many activations are transferred. The maximum size of the buffer required will be the size of all activations transferred from all devices. However, it is practical to establish a maximum buffer size and implement periodic updates to the buffer to efficiently manage its storage capacity. In addition, EcoFed stores the compressed activation outputs (z) instead of the original activations (a_k^t). The activation is compressed by the *Compressor* module of EcoFed using a lightweight 8-bit linear quantization technique [21] denoted as function $Q(\cdot)$. The output (a_k^t) is quantized from 32 bits to 8 bits before sending it to the server. The compressed activation (z_k^t) is then cached in the *Replay Buffer*.

Algorithm 1: Partitioning-based training in EcoFed

```

1 Input: Pre-trained  $w_C^*$  and data  $\{D_k\}_{k=1}^K$ 
2 Output:  $w^*$ 
3 for each device  $k \in K$  in parallel do
4   Download  $w_C^*$  to device  $k$ ;
5   Initialize and freeze  $w_{C,k}^*$ ;           //Pre-trained
                                         initialization
6 end
7 for each round (each device and corresponding worker
    $k \in K$  in parallel) do
8   Initialize  $w_{S,k}$  on the server;
9   for each round  $t \in T$  do
10    if Activation switch is on ( $t \bmod \rho == 0$ ) then
11      Forward on  $w_{C,k}^*$  to get  $a_k^t$ ;
12       $z_k^t \leftarrow Q(a_k^t)$ ;           //Quantization
13      Send  $z_k^t$  to the server;
14      update buffer with  $z_k^t$ ;
15    end
16    else
17       $z_k^t \leftarrow$  buffer;           //Replay Buffer
18    end
19     $\hat{a}_k^t \leftarrow Q^{-1}(z_k^t)$ ;       //Dequantization
20    Forward on  $w_{S,k}^t$ ;
21    Calculate loss  $\ell_{S,k}^t$  and gradients
        $\nabla \ell_{S,k}^t(w_{S,k}^t)$ ;
22     $w_{S,k}^t \leftarrow w_{S,k}^t - \eta \nabla \ell_{S,k}^t(w_{S,k}^t)$ ;
23  end
24   $w_{S,k} \leftarrow w_{S,k}^t$ ;
25   $w_S \leftarrow \sum_{k=1}^K \frac{|D_k|}{|D|} w_{S,k}$ ;           //FedAvg
26 end
27  $w_S^* \leftarrow w_S$ ;
28  $w^* \leftarrow \{w_C^*, w_S^*\}$ ;           //Concatenation of  $w_C^*$  and  $w_S^*$ 
29 return  $w^*$ 

```

2.4 Proposed Algorithm

Algorithm 1 shows the steps of partitioning-based training in EcoFed by employing pre-trained initialization and a replay buffer with compression using quantization.

We first present the notation used in EcoFed. The collection of K devices is denoted as $\{k\}_{k=1}^K$. Each device generates its own data D_k . The data from all devices is denoted as D : $\{D_k\}_{k=1}^K$. The number of samples in D_k is denoted as $|D_k|$ and the total number of samples is $|D|$. Let w be the entire model, which will be partitioned as the device-side model (w_C) and server-side model (w_S). $w_{C,k}$ and $w_{S,k}$ are the models of the k^{th} device. The superscript t is used to represent a training round t in a total of T rounds. a_k is the intermediate activation generated by $w_{C,k}$. $\ell_{S,k}(\cdot)$ is the loss function of the server-side model of the k^{th} device.

EcoFed first prepares the pre-trained weights of the device-side model (w_C^*). The weights of w_C^* will be frozen during training to eliminate the transfer of the gradient from the server-side to device-side model w_C (Lines 4 and 5). Then, the server-side model of each device will be trained independently with K parallel workers.

For each round t , if activation transfer is switched on (i.e. $t \bmod \rho == 0$), then the output activation of $w_{C,k}^*$ is

generated, denoted as a_k^t , and compressed to 8 bits, denoted as z_k^t . The compressed activation is uploaded to the edge server and is used to update the corresponding buffer (Lines 10-15). Alternatively, the edge server retrieves z_k^t directly from the buffer (Line 17). Using z_k^t , EcoFed will firstly dequantize z_k^t and provides the output \hat{a}_k^t to the server-side model for the training of $w_{S,k}$ (Lines 19-22).

Once a training round is completed by an edge server, it will send each $w_{S,k}$ to the cloud. The cloud aggregates a new global server-side model (Lines 24-26). Finally, after T rounds of training, the cloud obtains the optimal server-side model (w_S^*) and concatenates it with w_C^* into a complete model w^* (Lines 28-29).

3 CONVERGENCE AND COST ANALYSIS

In this section, we firstly analyze the convergence of EcoFed (Section 3.1). Then the computation and communication costs of EcoFed on the device-side are compared against classic FL, vanilla DPFL and local loss-based DPFL (Section 3.2).

3.1 Convergence Analysis

We follow the convergence analysis presented in the literature [10], [22], [23] to analyze the convergence of EcoFed (Algorithm 1). We assume the following:

Assumption 1 – The server-side objective functions are L -smooth, i.e., $\|\nabla F_S(u) - \nabla F_S(v)\| \leq L\|u - v\|, \forall u, \forall v$.

Assumption 2 – The squared norm of the stochastic gradient has an upper bound for the server-side object function, i.e., $\|\nabla F_S(a_k^t; w_{S,k}^t)\|^2 \leq G, \forall k, \forall t$.

Assumption 3 – The learning rate η_t satisfies $\sum_t \eta_t = \infty$ and $\sum_t \eta_t^2 < \infty$.

In each global round t , the output activation of the k_{th} device-side model is equal to $a_k^t = w_{C,k}^t(x)$. We assume a_k^t follows a probability distribution of $p_k^t(a)$, which is determined by w_C^t and D_k . In EcoFed, the device-side model $w_{C,k}^t$ is initialized with pre-trained weights and frozen during the training, thus fixed as $w_{C,k}^*$. In addition, EcoFed uses the quantization function $Q(\cdot)$ and dequantization function $Q^{-1}(\cdot)$ along with the *Replay Buffer* to train the server-side models, denoted as $\hat{a}_k^t \triangleq Q^{-1}(Q(a_k^t))$. We define the probability distributions of the *Replay Buffer* as $q_k^t(a)$.

To analyze the impact of *Replay Buffer* and quantization on the convergence, we further define two types of errors: buffer and quantization errors. Buffer error is defined as the distance of gradients between the original distribution $p_k^t(a)$ and buffer distribution $q_k^t(a)$, denoted as $\delta_k \triangleq \int \|\nabla \ell(a_k^t; w_S)\| \|q_k^t(a) - p_k^t(a)\| da$. The $\ell(\cdot)$ is the loss function (e.g. cross entropy loss for classification). Quantization error is defined as $\int \|\nabla \ell(\hat{a}_k^t; w_S) - \nabla \ell(a_k^t; w_S)\| \|q_k^t(a)\| da$, which is the sum of gradient errors over $q_k^t(a)$ due to quantization. We include a further assumption specific to EcoFed as follows:

Assumption 4 – The buffer error and the quantization error have upper bounds, i.e., $\delta_k^t \leq H_1$ and $\varepsilon_k^t \leq H_2, \forall k, \forall t$.

Convergence of device-side model: Since w_C is fixed during training in EcoFed, its convergence is not considered.

Convergence of server-side model: Let $\frac{1}{\Gamma_T} \triangleq \sum_{t=0}^{T-1} \eta_t$. Following on from Assumption 1, Assumption 2 and Assumption 4, Algorithm 1 ensures the following:

$$\frac{1}{\Gamma_T} \sum_{t=0}^{T-1} \eta_t \mathbb{E}[\|\nabla F_S(w_S^t)\|^2] \leq \frac{4(F_S(w_S^0) - F_S(w_S^*))}{3\Gamma_T} + \frac{1}{\Gamma_T} \sum_{t=0}^{T-1} \left(\eta_t(\sqrt{G} + 1)(H_1 + H_2) + \frac{L}{2} \eta_t^2 G \right) \quad (1)$$

where $\nabla F_S(w_S^t) \triangleq \frac{1}{K} \sum_{k=1}^K \nabla F_{S,k}(w_S^t)$. $F_{S,k}(\cdot)$ is the objective function of the k^{th} server-side model. w_S^0 is the initial server-side weights and w_S^* is the optimal server-side weights. The detailed proof is provided in Appendix A.

Based on Assumption 3, it is noted that with increasing T , the right-hand side of Equation 1 converges to zero. Thus, Equation 1 guarantees that the proposed algorithm of EcoFed converges to a stationary point with increasing T .

Differences between the convergence of local loss-based DPFL and EcoFed: Equation 1 is similar to the convergence analysis presented in the literature [10]. The server-side model converges as follows:

$$\frac{1}{\Gamma_T} \sum_{t=0}^{T-1} \eta_t \mathbb{E}[\|\nabla F_S(w_S^t)\|^2] \leq \frac{4(F_S(w_S^0) - F_S(w_S^*))}{3\Gamma_T} + G \frac{1}{\Gamma_T} \sum_{t=0}^{T-1} \left(\eta_t \frac{1}{K} \sum_{k=1}^K (d_k^t) + \frac{L}{2} \eta_t^2 \right) \quad (3)$$

where $d_k^t \triangleq \int \|p_k^t(a) - p_k^*(a)\| da$ which is defined as the distance between the probability distribution of activation a_k^t and a_k^* . It is worth noting that $p_k^t(a)$ keeps changing during FL training since $w_{C,k}^t$ is updated by the local error signals. Therefore, in local loss-based DPFL, the changing distance (d_k^t) of the probability distribution of a_k^t caused by updating $w_{C,k}^t$ affects the convergence of the server-side model as shown in Equation 3. However, in EcoFed, $d_k^t = 0$ since $w_{C,k}^t$ is fixed during training. In addition, the *Replay Buffer* and quantization error affects convergence behaviour, which is δ_k^t and ε_k^t (bounded by H_1 and H_2) as shown in Equation 1. Different ρ values and quantization techniques used by the *Compressor* module will determine the values of H_1 and H_2 , thus affecting the convergence of EcoFed.

3.2 Cost Analysis

Table 1 compares the computation and communication cost of EcoFed against classic FL, vanilla DPFL and local loss-based DPFL. We denote $|\cdot|$ as either the computation or communication workload of a given model or an activation. We distinguish two different modes in EcoFed, namely EcoFed without buffer and EcoFed with buffer. In classic FL, the entire model (w) is computed on each device ($|w|$). At the end of each round, w is uploaded to the cloud and then the newly aggregated w is downloaded to the device ($2|w|$). For vanilla DPFL, each device only needs to train the device-side model, w_C ($|w_C|$) and w_C is transferred at the end of each round ($2|w_C|$). In addition, the activation and gradient of each data sample will be communicated with an overhead of $2|D_k||a_k|$. For local loss-based DPFL, each device also requires to train w_C ($|w_C|$). In addition, w_C is uploaded and downloaded at the end of each round ($2|w_C|$).

TABLE 1: Computation and communication costs on the device for each round.

Methods	Computation	Communication
FL	$ w $	$2 w $
Vanilla DPFL	$ w_C $	$2 w_C + 2 D_k a_k $
Local loss-based DPFL	$ w_C $	$2 w_C + D_k a_k $
EcoFed w/o buffer	$\frac{1}{2} w_C $	$ D_k z_k $
EcoFed w buffer	0	0

but only the activation is transferred during training of each round ($|D_k||a_k|$).

However, for EcoFed without using the Replay Buffer (indicated as EcoFed w/o buffer; when the buffer is used indicated as EcoFed w buffer), the device only computes the forward pass on w_C , ($\frac{1}{2}|w_C|$). In addition, the communication overhead is reduced to $|D_k||z_k|$ where z_k is the compressed activation. There are no computation or communication costs during training when using the buffer.

4 EVALUATION

In this section, we evaluate EcoFed against four baselines using two sets of metrics. The test environment, the evaluation setup and the results obtained from the experimental studies are considered in this section. The results highlight that EcoFed improves accuracy compared to state-of-the-art methods and eliminates accuracy degradation caused by local error signals in local loss-based DPFL. In addition, EcoFed significantly reduces communication costs and accelerates training.

4.1 Test Environment

Datasets and Models: Two image classification datasets, namely CIFAR-10 [24] and CIFAR-100 [24] are used¹. We follow a similar method reported in the literature [13] to partition data across devices. For an independent and identically distributed (I.I.D.) setting, the training set is initially divided into 500 shards for CIFAR-10 and 5000 shards for CIFAR-100. We randomly assign 5 shards and 50 shards to each device for CIFAR-10 and CIFAR-100, respectively. In the non-I.I.D. setting, we first sort the dataset based on their labels, dividing it into 500 shards for CIFAR-10 and 5000 shards for CIFAR-100. Then, we randomly allocate 5 shards and 50 shards to each device for CIFAR-10 and CIFAR-100, respectively. Consequently, each device will have training samples of up to half of all available classes. The test dataset is available on the server and will be used to test model performance after each round of training.

We train two popular convolutional neural networks, namely VGG11 [27] (plain convolutional neural network) and ResNet9 [28] (residual convolutional neural network). For auxiliary networks used in local-based DPFL methods, we adopt a fully connected layer on each device as presented in the literature [10]. The architectures of VGG11, ResNet9 and the auxiliary network along with the device-side and server-side model partitions are shown in Table 2.

1. We do not report learning performance on MNIST [25] and FMNIST [26] as they are simple datasets and do not highlight the differences between the methods we evaluate.

TABLE 2: Models used for evaluation. Convolution layers denoted as C followed by the no. of filters; filter size is 3×3 for all convolution layers except for downsampling convolution (filter size is 1×1); MaxPooling layer is MP; Fully Connected layer is FC; and Residual Block is RB including two convolution layers, a max pooling and downsampling convolution layers; number followed is no. of output channels.

Model	Device	Server
VGG11	C64-MP-C128-MP	C256-C256-MP-C512-C512-MP-C512-C512-FC4096-FC4096-FC10
ResNet9	C64-MP-C128-MP	RB256-RB512-RB512-FC10
Auxiliary Network	FC10	N/A

FL Training hyper-parameters: At the beginning of each FL round, the server randomly selects 20 devices out of 100 devices (sampling ratio of 0.2) for participating in the current training round. The standard FedAvg [13] aggregation method is used by the *Aggregator* for all approaches. We adopt the same data augmentation and learning schedules for all methods for fair comparisons (horizontal flip with a probability of 0.5 and the Stochastic Gradient Descent (SGD) optimizer with a learning rate of 0.01). We set a total of 500 rounds for training on all datasets.

Testbed: To facilitate the evaluation of the system performance (i.e. communication cost and training latency), we build a prototype with an edge server and five resource constrained devices. The edge server has a 2.5GHz Intel i7 8-core CPU and 16GB RAM. Five Raspberry Pi 4 Model B single-board computers with 1.5GHz quad-core ARM Cortex-A53 CPU are used as representative of resource constrained devices. All devices and the server run the same training engine, namely PyTorch. The server and devices are connected to a router. We use Linux tc commands to emulate different network conditions of Wi-Fi (50/50 Mbps), 4G (10/42 Mbps) and 3G (3/6 Mbps) for different upload and download bandwidths.

We also employ a simulation-based test environment to evaluate the learning performance. The testbed is built on a 2GHz AMD EPYC 7713P 64-Core CPU with 252GB RAM and two Nvidia A6000 GPUs. This testing environment is used to facilitate a faster and more comprehensive evaluation of learning performance.

4.2 Evaluation Setup

Baselines: We consider four baselines, namely classic FL, SFL (vanilla DPFL) and two state-of-the-art local loss-based DPFL methods. They are:

1) **Classic FL** trains the entire model locally on each device.

2) **SFL (vanilla DPFL)** is the first DPFL approach. The model is partitioned into device-side and server-side models, which are sent to the devices and the server for training, respectively. The activation and gradient of the output of device-side model are transferred between devices and the server for each data batch. This method does not optimize communication.

3) **Local generated loss (LGL)** [10] introduces a locally generated loss on devices to generate gradients for training

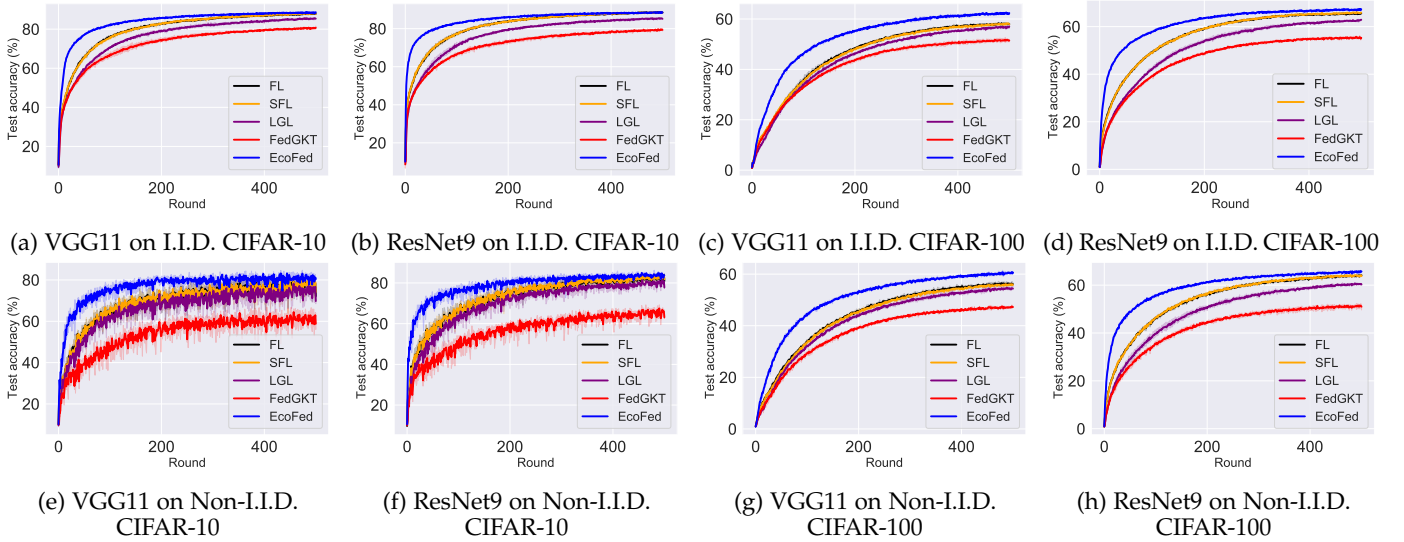


Fig. 4: Test accuracy curves of EcoFed and the baselines using VGG11 and ResNet9 in I.I.D. and Non-I.I.D. settings for CIFAR-10 and CIFAR-100 datasets.

TABLE 3: The highest test accuracy of EcoFed compared to the baselines for VGG11 and ResNet9 on two datasets on I.I.D. and Non-I.I.D. distribution. The results are an average of three independent runs with different random seeds.

Methods	CIFAR-10				CIFAR-100			
	I.I.D.		Non-I.I.D.		I.I.D.		Non-I.I.D.	
	VGG11	ResNet9	VGG11	ResNet9	VGG11	ResNet9	VGG11	ResNet9
FL	88.29%	88.95%	82.01%	84.52%	58.48%	65.87%	56.79%	64.29%
SFL	88.31%	88.81%	81.38%	84.56%	58.5%	66.32%	56.47%	64.42%
LGL	85.76%	85.65%	79.66%	82.18%	57.22%	63.01%	54.88%	61%
FedGKT	81.09%	79.82%	66.39%	68.71%	52.03%	55.92%	47.74%	51.81%
EcoFed	88.87%	88.81%	84.47%	85.82%	62.81%	67.61%	61.1%	66.08%

the device-side model, thus reducing the need for transmission of gradients from the server.

4) **FedGKT** [11] also incorporates local loss on devices. In addition, probabilistic predictions, called soft labels [29], of the server-side models are periodically transferred to the devices and vice versa. The soft labels are used to distill the training of device-side models and server-side models².

5) **EcoFed** is implemented with following configuration. We adopt the pre-trained weights of the device-side model from the respective pre-trained model trained on the ImageNet dataset [19] and freeze them during the training. $\rho = 2$ for the *Replay Buffer* (the buffer will be updated every two rounds). In addition, a linear 8-bit quantization implementation is adopted for the *Compressor*.

Evaluation Metrics: Two sets of metrics are used to evaluate performance. They are:

1) **Metrics on learning performance:** (i) *Accuracy* is evaluated on the global test data. We record the highest test accuracy achieved during entire rounds of training for each baseline. The results are an average of three independent runs with different random seeds.

2) **Metrics on system performance:** (i) *Communication cost* is the measured communication overhead for one round. The communication cost versus test accuracy curve is presented to evaluate the efficiency of communication for achieving a target accuracy; (ii) *Training latency* is the wall-

clock time of one training round for each baseline given a network bandwidth.

4.3 Accuracy

The test accuracy curves of the five methods, including EcoFed and the four baseline methods, on the two datasets (both I.I.D. and Non-I.I.D. setting) using the two DNN models are shown in Figure 4. In addition, the highest test accuracy is reported in Table 3. The results show that EcoFed usually outperforms all baselines across all datasets and the two model architectures (except for FL on I.I.D. CIFAR-10 for ResNet9). In detail, EcoFed achieves up to a 4.63% increase in accuracy on Non-I.I.D. CIFAR-100 for VGG11 compared to SFL (4.31% compared to FL). In addition, EcoFed significantly improves the accuracy by up to 6.22% on Non-I.I.D. CIFAR-100 for VGG11 compared to LGL and by up to 18.08% on Non-I.I.D. CIFAR-10 for VGG11 compared to FedGKT, respectively.

SFL offloads parts of the training computation to the server but fundamentally shares the same algorithm as FL. As a result, their accuracy and learning curves are similar. LGL and FedGKT introduce local error signals to reduce communication. However, although there is a reduction in communication, there is a significant loss in accuracy and slower convergence speed compared to FL and SFL. EcoFed, on the other hand, does not have an accuracy degradation commonly seen in LGL and FedGKT, while also achieving a more substantial reduction in communication

² The implementation of FedGKT for our experiments is a variant that we developed based on vanilla DPFL in order to compare it to other baselines when using the same aggregation algorithm, i.e., FedAvg.

TABLE 4: The highest test accuracy of FedGKT (bi-direction) and FedGKT (uni-direction) on CIFAR-10. The results are an average of three independent runs with different random seeds.

FedGKT	I.I.D.		Non-I.I.D.	
	VGG11	ResNet9	VGG11	ResNet9
Bidirection	81.09%	79.82%	66.39%	68.71%
Unidirection	83.18%	83.42%	75.89%	77.68%

TABLE 5: The highest test accuracy of EcoFed compared to the baselines on CIFAR-10 with pre-trained initialization on the device-side model. The results are an average of three independent runs with different random seeds.

Methods	I.I.D.		Non-I.I.D.	
	VGG11	ResNet9	VGG11	ResNet9
FL	89.48%	89.55%	84.81%	86.06%
SFL	89.44%	89.57%	85.02%	86.19%
LGL	88.06%	88.29%	83.44%	85.04%
FedGKT	83.59%	82.35%	72.73%	74.36%
EcoFed	88.87%	88.81%	84.47%	85.82%

costs compared to local loss-based DPFL methods (Section 4.4).

4.3.1 Impact of pre-trained initialization and freezing weights on the device-side model

To obtain a better understanding of accuracy achieved in Figure 4 and Table 3, we further investigate accuracy degradation in local loss-based DPFL methods and the effects of using pre-trained initialization and freezing weights on w_c in EcoFed. We answer the following three questions³:

Can local error signals generated on the device degrade accuracy? From Table 3 and Figure 4, it is noted that local loss-based DPFL methods suffer a higher accuracy loss than the other methods. Even when compared to FL and SFL, LGL and FedGKT consistently achieve lower accuracy. In addition, local loss-based DPFL has a slower convergence rate as demonstrated in Figure 4 resulting from separately optimizing the device-side model and the server-side model by inconsistent gradient signals.

In addition, we notice that FedGKT has a relatively lower accuracy compared to LGL. In FedGKT, knowledge distillation is carried out both on device-side and server-side models. We demonstrate that the distillation of device-side soft labels on server-side training has a negative impact on accuracy. Table 4 shows the accuracy results of bidirectional FedGKT and unidirectional FedGKT (only the server-side soft labels are used for distilling the device-side model). We observe a significant accuracy improvement when removing distillation from device-side soft labels when training the server-side model, shown as unidirectional FedGKT. This further demonstrates that local training results in the accuracy degradation of the server-side model.

Can pre-trained initialization on the device-side model also improve accuracy for other baselines? We further investigate the impact of pre-trained initialization of the device-side model for FL, SFL and local loss-based DPFL methods. Table 5 shows the highest test accuracy achieved by each method when we apply pre-trained initialization for

TABLE 6: The highest test accuracy of device-side model of trainable w_c and frozen w_c^* in LGL (on CIFAR-10) and the highest test accuracy of respective server-side models under w_c and w_c^* . The results are an average of three independent runs with different random seeds.

	LGL	I.I.D.		Non-I.I.D.	
		VGG11	ResNet9	VGG11	ResNet9
Device	Trainable w_c	78.61%	78.68%	76.78%	76.77%
	Frozen w_c^*	70.6%	70.72%	69.46%	67.89%
Server	w_s under w_c	87.82%	88.04%	83.05%	84.9%
	w_s under w_c^*	88.97%	89.34%	84.4%	85.77%

the device-side model. The results indicate that pre-trained initialization can significantly improve the accuracy of FL and SFL, specifically in the Non-I.I.D. setting. This finding has also been observed in recent research [30], [31].

Surprisingly, the results demonstrate that pre-trained initialization can also mitigate accuracy degradation caused by local error signals in the local loss-based DPFL methods, which to the best of our knowledge, has never been reported before. When all methods adopt pre-training initialization, EcoFed still outperforms all local loss-based DPFL methods. Compared to FL and SFL, EcoFed achieves competitive accuracy performance (less than 1% loss) with considerable communication reduction by up to 114x (Section 4.4).

Does training the device-side models with local loss in the context of pre-trained initialization improve the accuracy of the server-side model? In LGL and FedGKT, the device-side model is trained by local error signals to avoid the need for receiving gradients. However, in the context of pre-trained initialization, we investigate whether device-side training by local loss can improve the training of server-side model after applying pre-trained initialization on the device-side model.

To this end, the test accuracy of device-side model (w_c) and server-side model (w_s) of LGL are recorded on CIFAR-10. We compare the test accuracy of LGL (with pre-trained initialization) with trainable w_c (device-side model) and frozen w_c^* . Table 6 shows that the trainable w_c has significantly higher test accuracy than the frozen w_c^* across I.I.D. and Non-I.I.D. settings. However, in terms of server-side model (w_s), it is surprising that the server-side model when the device-side model is frozen (denoted as w_s under w_c^*) achieves higher accuracy compared to the server-side model with a trainable device-side model (denoted as w_s under w_c).

The results suggest that training the device-side model can indeed significantly improve the accuracy of the device-side model, but it does not necessarily improve the accuracy of the server-side model and may even degrade the accuracy of the server-side model. However, the accuracy of the server-side model is what we ultimately aim to achieve. It is thus inferred that local training on the device-side model is not required for improving the accuracy performance of server-side model. We conjecture that the local error signals generated by the local auxiliary network are not optimal for the training performance of server-side models. Given the above observations, EcoFed freezes the device-side weights when pre-trained initialization is adopted.

3. Due to the limitation of space, we only show the results for CIFAR-10. However, the same conclusions were observed for CIFAR-100.

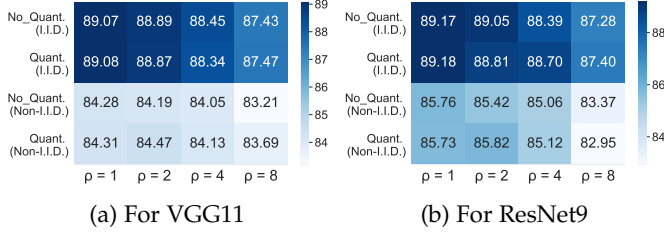


Fig. 5: Accuracy for different ρ values with or without quantization in EcoFed. The results are an average of three independent runs with different random seeds.

4.3.2 Impact of ρ and quantization on accuracy

We investigate the accuracy performance of EcoFed under different hyper-parameters setting. ρ controls the update frequency of the *Replay Buffer* and quantization is adopted to reduce the size of transferred data and consequently, the memory required by the cached buffer. The impact of ρ and quantization on test accuracy for CIFAR-10 is shown in Figure 5. In general, the accuracy gradually decreases as ρ increases since the update frequency is reduced. Accuracy is less sensitive to quantization since (near) similar accuracy is achieved with or without quantization for the same ρ value. It is worth noting that when $\rho = 1$, EcoFed updates the cached buffer every round.

4.4 Communication Cost

Communication cost for one training round: The communication overhead of EcoFed and the four baselines methods are compared for one training round on the CIFAR-10 dataset⁴. Communication costs incurred between the devices and server for EcoFed and others baselines are shown in Table 7.

Compared to classic FL, other DPFL methods have a smaller communication overhead; for example, the communication cost is reduced by 8.27x (SFL) and 15.55x (LGL and FedGKT) when training VGG11. The reason is that DPFL methods only need to transfer the device-side model between the devices and the server, which is usually smaller in size than the entire model. It is to be noted that EcoFed (with buffer) achieves a further reduction in communication cost of 57x on VGG11 and 15.56x on ResNet9. When using the buffer, EcoFed fundamentally eliminates the need for communication. In terms of the overall communication costs for all rounds of FL, EcoFed ($\rho = 2$) can reduce communication by 114x on VGG11 and 31.12x on ResNet9 compared to classic FL.

Compared to the other DPFL methods, EcoFed also reduces the communication cost significantly. EcoFed without buffer reduces the communication cost by 6.89x, 3.67x and 3.67x on both VGG11 and ResNet9. LGL and FedGKT can reduce the communication cost by half when compared to SFL as they only require the activations to be transferred from devices to the server. However, due to the cached buffer technique in EcoFed, the average communication per

TABLE 7: Communication cost for one training round.

Methods	Communication cost	
	VGG11	ResNet9
FL	5.13 GB	1.4 GB
SFL	0.62 GB	0.62 GB
LGL	0.33 GB	0.33 GB
FedGKT	0.33 GB	0.33 GB
EcoFed w/o buffer	0.09 GB	0.09 GB
EcoFed w buffer	0 GB	0 GB

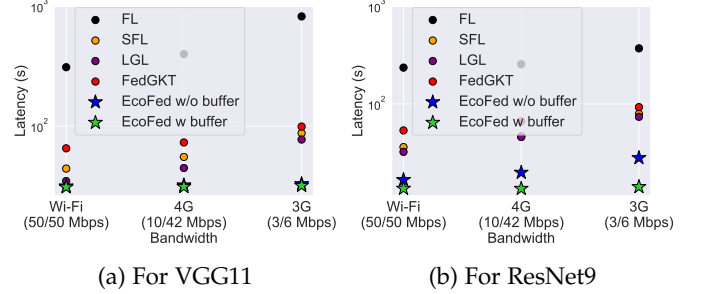


Fig. 6: Latency of one training round for VGG11 and ResNet9 under different network conditions. The results are an average of three independent runs.

round is further reduced by a factor of ρ . For instance, in our experiments with $\rho = 2$, the average communication per round is 0.045 GB, which is 13.78x, 7.34x and 7.34x lower than SFL, LGL and FedGKT, respectively.

Communication cost vs test accuracy: The cumulative communication cost for all training rounds on the two datasets is considered. The communication cost after each training round is recorded. Figure 7 highlights the communication cost incurred to achieve a target test accuracy.

For instance, given a test accuracy target of 80% on I.I.D. CIFAR-10 for VGG11, FL, SFL, LGL and FedGKT will require 729 GB, 90 GB, 71 GB and 145 GB of data transfers, respectively. Similarly, for a 50% test accuracy target on I.I.D. CIFAR-100 the communication costs for VGG11 are 1121 GB, 139 GB, 110 GB and 156 GB on I.I.D. CIFAR-100. However, EcoFed will only require 4 GB on I.I.D. CIFAR-10 and 7 GB on I.I.D. CIFAR-100 to achieve the target test accuracy. For ResNet9, FL, SFL, and LGL will require 169 GB, 78 GB, and 67 GB of data to be transferred (150 GB, 65 GB, 64 GB and 100 GB on I.I.D. CIFAR-100), respectively. FedGKT fails to achieve 80% test accuracy on I.I.D. CIFAR-10 and requires 100 GB on I.I.D. CIFAR-100 for 50% test accuracy. In contrast, EcoFed has a significantly low volume of data transfer 4 GB on I.I.D. CIFAR-10 (3 GB on I.I.D. CIFAR-100) to achieve the target test accuracy.

For the Non-I.I.D. setting on both datasets, EcoFed has higher communication efficiency to reach a target test accuracy when compared to all baselines. It is worth noting that although the communication of LGL and FedGKT is reduced by half per round (since gradient transfers are eliminated) compared to SFL, the volume of communication required to achieve the same level of accuracy does not significantly decrease, and in some cases, such as ResNet9 on CIFAR-100 increases. This is because of accuracy degradation and slower convergence using local error signals.

EcoFed reduces the communication cost by 114x on VGG11 (31.11x on ResNet9) compared to classic FL. Com-

4. For the results evaluating communication cost and training latency of one training round, we only report the results on the CIFAR-10 dataset as the system performance is independent of the datasets we considered.

pared to SFL (vanilla DPFL), EcoFed improves communication by up to 13.78x. In short, classic FL, SFL (vanilla DPFL) and even local loss-based DPFL still incur significant communication costs. However, EcoFed has significantly lower communication costs and higher communication efficiency.

4.5 Training Latency

Improving the communication efficiency by reducing the transmission frequency and size of data transferred by EcoFed results in a speedup of the overall training latency. To quantify this benefit, the average training time for one round of EcoFed is compared against the baseline methods. Figure 6a and Figure 6b highlight that compared to classic FL, EcoFed achieves a 9.87x and 14.16x speed up for VGG11 and ResNet9 without using buffer (under Wi-Fi conditions), respectively. In addition, compared to SFL (vanilla DPFL), EcoFed achieves a speedup of 1.4x and 2.17x on VGG11 and ResNet9 without using the buffer (under Wi-Fi conditions). Compared to local loss-based DPFL methods (LGL and FedGKT) with communication optimization, there is an improvement of training latency of about 1.1x and 2.07x on VGG11 and 1.94x and 3.21x on ResNet9 without using the buffer.

We further consider the impact of network bandwidth, which will be a bottleneck for devices that operate in environments that have limited network capabilities (e.g. mobile phones with 4G or 3G signal). Therefore, we evaluated EcoFed and each baseline under different network bandwidth conditions. When the network bandwidth is limited to 4G (10 Mbps and 42 Mbps for upload and download) and 3G (3 Mbps and 6 Mbps for upload and download), the training latency of FL, SFL, LGL and FedGKT are high due to the increase in the communication costs for transferring the model and intermediate activation and gradients. It is worth noting that local loss-based methods (i.e. LGL and FedGKT) have a similar training latency compared to non-optimized vanilla DPFL (i.e. SFL) when the network bandwidth is limited to 3G since they still incur large communication costs due to transferring activations. In addition, the upload bandwidth for sending activations is typically lower than the download bandwidth used for sending gradients, and it has not been considered in local loss-based DPFL. This highlights the importance of reducing communication costs when transferring activations.

However, EcoFed only has a small increase in training latency, resulting in a 25.11x and 2.66x speed up on VGG11 and 13.29x and 2.83x speed up on ResNet9 in a 3G network, compared to FL and SFL, respectively. In addition, when EcoFed employs the buffer for training (half of the entire rounds when $\rho = 2$), the training latency is fundamentally independent of network bandwidths. This further demonstrates the merit of EcoFed in terms of its low bandwidth requirements.

5 RELATED WORK

In this section, we consider the literature on DPFL methods, techniques used for reducing communication in FL, the concept of pre-training in FL, and layer-wise learning.

DPFL: Existing research on DPFL can be categorized as vanilla DPFL and local loss-based DPFL. SFL [12] partitions a DNN across the device and the server in FL. FL and split learning [32] are combined such that the device-side models are independently trained by receiving gradients from the server. The server-side models are trained by collecting activations from devices in parallel. SFL alleviates the computational burden on resource constrained devices and accelerates training. However, SFL does not consider the communication overhead introduced by DNN partitioning.

Recently DPFL approaches have been optimized by computing local loss on the device-side to reduce the communication cost [10], [11]. In these approaches, the device-side model is trained with local error signals generated by an additional auxiliary network. This eliminates the need for transferring the gradient from the server and making use of it on the device. However, the training of device-side model with local error signals is sub-optimal, thus detrimental to accuracy. In addition, the communication costs to transfer the activation are not considered. One drawback of DPFL methods is the vulnerability of activations to hacking, including model inversion attacks that can potentially recover the original data [33]. However, a potential solution is to incorporate homomorphic encryption to encode the activation of the device-side model to secure communication in DPFL [34].

Communication Reduction in FL: Communication reduction techniques in FL can be grouped into two categories, depending on whether (i) they reduce the frequency of communication or (ii) compress the size of the transferred data. Under the first category, a key technique is to increase the interval between model aggregation, thus reducing the communication frequency from the device to the server and vice-versa [35]–[37]. Under the second category, compression approaches, such as quantization and sparsification, are employed to minimize the size of models (updated weights) in each round of communication [38], [39]. However, the above focus on the communication of the updated models at the end of each FL round, rather than the communication costs introduced due to DNN partitioning during training, which this paper considers.

Pre-training in FL: Pre-training a model is rarely investigated in the literature on FL. Instead, the model is usually trained from random weights. Recent work has demonstrated that pre-training can close the accuracy gap between FL and centralized learning, specifically in the non-IID setting [30], [31]. This paper utilizes pre-training on the device-side and presents an approach to reduce the accuracy loss inherent to local loss-based DPFL methods; both of these are considered for the first time.

Layer-wise Learning: Another line of related research is layer-wise learning in which each DNN layer is independently trained using auxiliary networks [18], [22], [40]. Since these approaches train using local loss in a resource-rich environment (with centralized servers that have an abundance of resources), the computation overheads of each layer and communication costs to transfer intermediate data are rarely considered. EcoFed can be considered as a special case of parallel block-wise learning. However, the device-side model is deployed in a resource-constrained environment

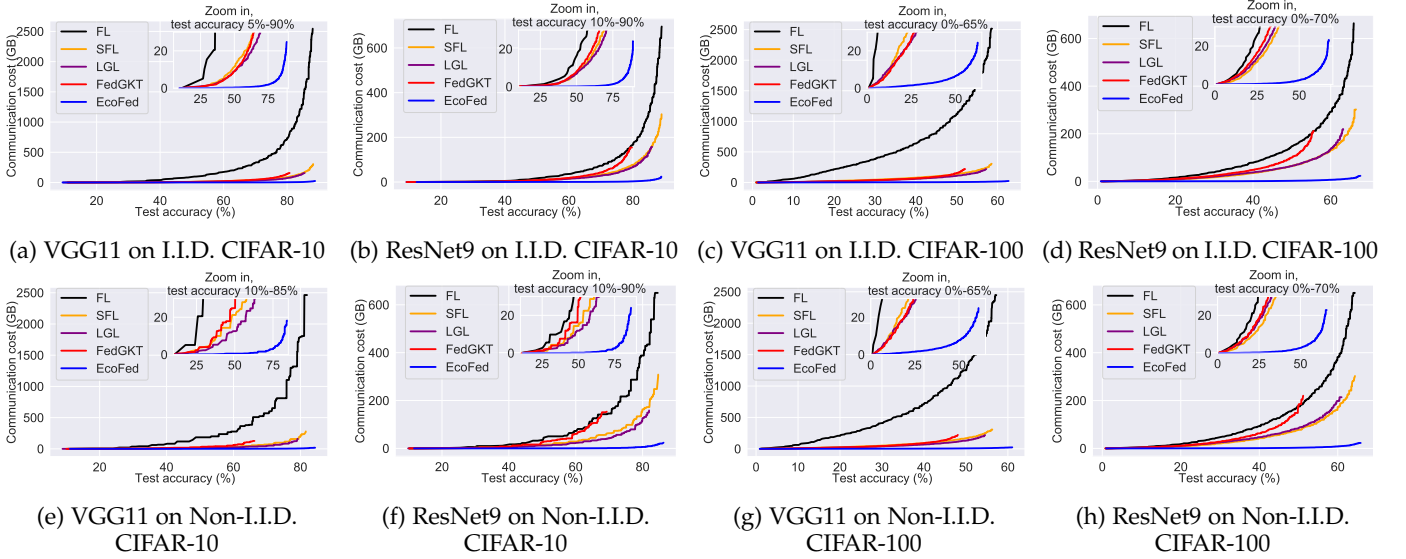


Fig. 7: Communication cost versus test accuracy of VGG11 and ResNet9 for the I.I.D. and Non-I.I.D. settings on CIFAR-10 and CIFAR-100 datasets.

on devices with limited computation and communication resources, which is challenging.

6 CONCLUSION

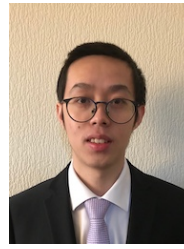
In this paper, we presents EcoFed, a communication-efficient DNN partitioning-based federated learning (DPFL) framework. DPFL partitions a DNN and offloads some of the layers of the DNN (or computation) from a resource constrained device to the server. EcoFed proposes pre-trained initialization to eliminate the transmission of the gradient from the server-side model to device-side model in DPFL for the first time and designs a novel replay buffer mechanism with quantization-based compression to further reduce the communication cost incurred by transferring activation. In other words, EcoFed proposes a unique way of carrying out the forward and backward passes for efficiently training in resource constrained environments. We comprehensively evaluate EcoFed and demonstrate that EcoFed can reduce the accuracy degradation caused by state-of-the-art local loss-based DPFL methods while significantly improve the communication efficiency and training speed compared to classical FL and state-of-the-art DPFL methods.

REFERENCES

- [1] A. Hard, K. Rao, R. Mathews, S. Ramaswamy, F. Beaufays, S. Augenstein, H. Eichner, C. Kiddon, and D. Ramage, "Federated Learning for Mobile Keyboard Prediction," *arXiv preprint arXiv:1811.03604*, 2018.
- [2] S. Ramaswamy, R. Mathews, K. Rao, and F. Beaufays, "Federated Learning for Emoji Prediction in a Mobile Keyboard," *arXiv preprint arXiv:1906.04329*, 2019.
- [3] D. Leroy, A. Coucke, T. Lavril, T. Gisselbrecht, and J. Dureau, "Federated Learning for Keyword Spotting," in *2019 IEEE International Conference on Acoustics, Speech and Signal Processing*, 2019, pp. 6341–6345.
- [4] A. Imteaj, K. Mamun Ahmed, U. Thakker, S. Wang, J. Li, and M. H. Amini, *Federated Learning for Resource-Constrained IoT Devices: Panoramas and State of the Art*. Springer International Publishing, 2023, pp. 7–27.
- [5] D. C. Nguyen, M. Ding, P. N. Pathirana, A. Seneviratne, J. Li, and H. V. Poor, "Federated learning for Internet of Things: A Comprehensive Survey," *IEEE Communications Surveys & Tutorials*, vol. 23, no. 3, pp. 1622–1658, 2021.
- [6] Y. Gao, M. Kim, S. Abuadbbba, Y. Kim, C. Thapa, K. Kim, S. A. Camtepe, H. Kim, and S. Nepal, "End-to-End Evaluation of Federated Learning and Split Learning for Internet of Things," in *International Symposium on Reliable Distributed Systems*, 2020, pp. 91–100.
- [7] C. Wang, Y. Yang, and P. Zhou, "Towards Efficient Scheduling of Federated Mobile Devices under Computational and Statistical Heterogeneity," *IEEE Transactions on Parallel and Distributed Systems*, vol. 32, no. 2, pp. 394–410, 2021.
- [8] Z. Xu, F. Yu, J. Xiong, and X. Chen, "Helios: Heterogeneity-Aware Federated Learning with Dynamically Balanced Collaboration," in *ACM/IEEE Design Automation Conference*, 2021, pp. 997–1002.
- [9] D. Wu, R. Ullah, P. Harvey, P. Kilpatrick, I. Spence, and B. Varghese, "FedAdapt: Adaptive Offloading for IoT Devices in Federated Learning," *IEEE Internet of Things Journal*, 2022.
- [10] D.-J. Han, H. I. Bhatti, J. Lee, and J. Moon, "Accelerating Federated Learning with Split Learning on Locally Generated Losses," in *International Conference on Machine Learning Workshop on Federated Learning for User Privacy and Data Confidentiality*, 2021.
- [11] C. He, M. Annavaram, and S. Avestimehr, "Group Knowledge Transfer: Federated Learning of Large CNNs at the Edge," *Advances in Neural Information Processing Systems*, vol. 33, 2020.
- [12] C. Thapa, P. C. M. Arachchige, S. Camtepe, and L. Sun, "SplitFed: When Federated Learning Meets Split Learning," in *AAAI Conference on Artificial Intelligence*, vol. 36, no. 8, 2022, pp. 8485–8493.
- [13] B. McMahan, E. Moore, D. Ramage, S. Hampson, and B. A. y Arca, "Communication-Efficient Learning of Deep Networks from Decentralized Data," in *Proceedings of the International Conference on Artificial Intelligence and Statistics*, 2017, pp. 1273–1282.
- [14] S. Han, H. Mao, and W. J. Dally, "Deep Compression: Compressing Deep Neural Networks with Pruning, Trained Quantization and Huffman Coding," *arXiv preprint arXiv:1510.00149*, 2015.
- [15] J. Yang, X. Shen, J. Xing, X. Tian, H. Li, B. Deng, J. Huang, and X.-s. Hua, "Quantization Networks," in *IEEE/CVF Conference on Computer Vision and Pattern Recognition*, 2019, pp. 7308–7316.
- [16] Y. Choukroun, E. Kravchik, F. Yang, and P. Kisilev, "Low-bit Quantization of Neural Networks for Efficient Inference," in *IEEE/CVF International Conference on Computer Vision Workshop*, 2019, pp. 3009–3018.
- [17] D.-J. Han, D.-Y. Kim, M. Choi, C. G. Brinton, and J. Moon, "SplitGP: Achieving Both Generalization and Personalization in Federated Learning," *arXiv preprint arXiv:2212.08343*, 2022.
- [18] E. Belilovsky, M. Eickenberg, and E. Oyallon, "Greedy Layerwise

Learning Can Scale To Imagenet,” in *International Conference on Machine Learning*, 2019, pp. 583–593.

- [19] J. Deng, W. Dong, R. Socher, L.-J. Li, K. Li, and L. Fei-Fei, “Imagenet: A Large-Scale Hierarchical Image Database,” in *IEEE Conference on Computer Vision and Pattern Recognition*, 2009, pp. 248–255.
- [20] J. Yosinski, J. Clune, Y. Bengio, and H. Lipson, “How Transferable are Features in Deep Neural Networks?” *Advances in Neural Information Processing Systems*, vol. 27, 2014.
- [21] D. Wu, Q. Tang, Y. Zhao, M. Zhang, Y. Fu, and D. Zhang, “EasyQuant: Post-Training Quantization via Scale Optimization,” *arXiv preprint arXiv:2006.16669*, 2020.
- [22] E. Belilovsky, M. Eickenberg, and E. Oyallon, “Decoupled Greedy Learning of CNNs,” in *International Conference on Machine Learning*, 2020, pp. 736–745.
- [23] J. Wang, H. Qi, A. S. Rawat, S. Reddi, S. Waghmare, F. X. Yu, and G. Joshi, “FedLite: A Scalable Approach for Federated Learning on Resource-constrained Clients,” *arXiv preprint arXiv:2201.11865*, 2022.
- [24] A. Krizhevsky, G. Hinton *et al.*, “Learning Multiple Layers of Features from Tiny Images,” Technical report, 2009.
- [25] Y. LeCun, L. Bottou, Y. Bengio, and P. Haffner, “Gradient-based Learning Applied to Document Recognition,” *Proceedings of the IEEE*, vol. 86, no. 11, pp. 2278–2324, 1998.
- [26] H. Xiao, K. Rasul, and R. Vollgraf, “Fashion-Mnist: A Novel Image Dataset for Benchmarking Machine Learning Algorithms,” *arXiv preprint arXiv:1708.07747*, 2017.
- [27] K. Simonyan and A. Zisserman, “Very Deep Convolutional Networks for Large-Scale Image Recognition,” *arXiv:1409.1556*, 2014.
- [28] K. He, X. Zhang, S. Ren, and J. Sun, “Deep Residual Learning for Image Recognition,” in *IEEE Conference on Computer Vision and Pattern Recognition*, 2016, pp. 770–778.
- [29] G. Hinton, O. Vinyals, J. Dean *et al.*, “Distilling the Knowledge in A Neural Network,” *arXiv preprint arXiv:1503.02531*, vol. 2, no. 7, 2015.
- [30] H.-Y. Chen, C.-H. Tu, Z. Li, H.-W. Shen, and W.-L. Chao, “On Pre-Training for Federated Learning,” *arXiv preprint arXiv:2206.11488*, 2022.
- [31] J. Nguyen, K. Malik, M. Sanjabi, and M. Rabbat, “Where to Begin? Exploring the Impact of Pre-Training and Initialization in Federated Learning,” *arXiv preprint arXiv:2206.15387*, 2022.
- [32] P. Vepakomma, O. Gupta, T. Swedish, and R. Raskar, “Split Learning for Health: Distributed Deep Learning Without Sharing Raw Patient Data,” *arXiv:1812.00564*, 2018.
- [33] A. Mahendran and A. Vedaldi, “Understanding Deep Image Representations by Inverting Them,” in *IEEE Conference on Computer Vision and Pattern Recognition*, 2015.
- [34] K. Cheng, T. Fan, Y. Jin, Y. Liu, T. Chen, D. Papadopoulos, and Q. Yang, “Secureboost: A Lossless Federated Learning Framework,” *IEEE Intelligent Systems*, vol. 36, no. 6, pp. 87–98, 2021.
- [35] S. Wang, T. Tuor, T. Salonidis, K. K. Leung, C. Makaya, T. He, and K. Chan, “Adaptive Federated Learning in Resource Constrained Edge Computing Systems,” *IEEE Journal on Selected Areas in Communications*, vol. 37, no. 6, pp. 1205–1221, 2019.
- [36] X. Wu, X. Yao, and C.-L. Wang, “FedSCR: Structure-based communication reduction for federated learning,” *IEEE Transactions on Parallel and Distributed Systems*, vol. 32, no. 7, pp. 1565–1577, 2020.
- [37] Q. Wu, X. Chen, T. Ouyang, Z. Zhou, X. Zhang, S. Yang, and J. Zhang, “HiFlash: Communication-Efficient Hierarchical Federated Learning with Adaptive Staleness Control and Heterogeneity-aware Client-Edge Association,” *IEEE Transactions on Parallel and Distributed Systems*, 2023.
- [38] A. Reisizadeh, A. Mokhtari, H. Hassani, A. Jadbabaie, and R. Pedarsani, “FedpPAQ: A Communication-Efficient Federated Learning Method with Periodic Averaging and Quantization,” in *Proceedings of the International Conference on Artificial Intelligence and Statistics*, 2020, pp. 2021–2031.
- [39] P. Han, S. Wang, and K. K. Leung, “Adaptive Gradient Sparsification for Efficient Federated Learning: An Online Learning Approach,” in *IEEE International Conference on Distributed Computing Systems*, 2020, pp. 300–310.
- [40] A. Nøkland and L. H. Eidnes, “Training Neural Networks with Local Error Signals,” in *International Conference on Machine Learning*, 2019, pp. 4839–4850.



Di Wu is currently pursuing a PhD degree in computer science at University of St Andrews, UK. He received a B.S. degree in Information System and Information Management from Northeast Forestry University, China in 2015, and an M.S. degree in Data Science from University of Southampton, UK in 2018. His major interests are in the areas of federated learning, distributed machine learning, edge computing, model compression, and Internet-of-Things.



learning for edge computing systems. More information is available from www.rehmatkhan.com.

Rehmat Ullah earned a PhD degree in electronics and computer engineering from Hongik University, South Korea. He is currently an Assistant Professor at the Cardiff School of Technologies, Cardiff Metropolitan University, UK. Previously, he worked as a research fellow at University of St Andrews, UK and as an assistant professor at Gachon University, South Korea. His research interests are in edge computing, information centric networking and 5G evolution and beyond with a recent focus on federated



Philip Rodgers received the PhD degree in Computer Science from the University of Strathclyde, UK in 2019. He is currently a Research Scientist at the Rakuten Mobile Innovation Studio, Japan. His research interests are in distributed algorithms for artificial intelligence.



Peter Kilpatrick received the PhD degree in Computer Science in 1985, and the BSc degree in Mathematics and Computer Science in 1981. He is currently a Reader in Computer Science at Queen's University Belfast. His interests include parallel programming models and cloud and edge computing.



Ivor Spence received the PhD degree in computer science from Queen's University Belfast, UK, where he did research on code generation. He is currently a Reader in computer science at Queen's University Belfast where he leads the artificial intelligence (AI) research theme. His research is primarily on heterogeneous computing systems for AI.



Blesson Varghese received the PhD degree in Computer Science from the University of Reading, UK on international scholarships. He is a Reader in Computer Science at the University of St Andrews, UK, and the Principal Investigator of the Edge Computing Hub. He is a previous Royal Society Short Industry Fellow. His interests include distributed systems that span the cloud-edge-device continuum and edge intelligence applications. More information is available from www.blessonv.com.